Original Article

Effects of extracellular vesicles from mesenchymal stem cells on oxygen-glucose deprivation/reperfusion-induced neuronal injury

Shuang-shuang Gu[1], Xiu-wen Kang[1,2], Jun Wang[2], Xiao-fang Guo[1], Hao Sun[1], Lei Jiang[1], Jin-song Zhang[1]

[1] *Department of Emergency, the First Affiliated Hospital of Nanjing Medical University, Nanjing 210029, China*
[2] *Key Laboratory of Modern Toxicology, Ministry of Education, Department of Toxicology, School of Public Health, Nanjing Medical University, Nanjing 211166, China*

Corresponding Author: *Jin-song Zhang, Email: zhangjso@njmu.edu.cn; Lei Jiang, Email: racheljl@126.com*

BACKGROUND: Small extracellular vesicles (sEVs) from bone marrow mesenchymal stem cells (BMSCs) have shown therapeutic potential for cerebral ischemic diseases. However, the mechanisms by which BMSC-derived sEVs (BMSC-sEVs) protect neurons against cerebral ischemia/reperfusion (I/R) injury remain unclear. In this study, we explored the neuroprotective effects of BMSC-sEVs in the primary culture of rat cortical neurons exposed to oxygen-glucose deprivation and reperfusion (OGD/R) injury.

METHODS: The primary cortical neuron OGD/R model was established to simulate the process of cerebral I/R *in vitro*. Based on this model, we examined whether the mechanism through which BMSC-sEVs could rescue OGD/R-induced neuronal injury.

RESULTS: BMSC-sEVs (20 μg/mL, 40 μg/mL) significantly decreased the reactive oxygen species (ROS) productions, and increased the activities of superoxide dismutase (SOD) and glutathione peroxidase (GPx). Additionally, BMSC-sEVs prevented OGD/R-induced neuronal apoptosis *in vivo*, as indicated by increased cell viability, reduced lactate dehydrogenase (LDH) leakage, decreased terminal deoxynucleotidyl transferase (TdT)-mediated dUTP nick end labeling (TUNEL) staining-positive cells, down-regulated cleaved caspase-3, and up-regulated Bcl-2/Bax ratio. Furthermore, Western blot and flow cytometry analysis indicated that BMSC-sEV treatment decreased the expression of phosphorylated calcium/calmodulin-dependent kinase II (p-CaMK II)/CaMK II, suppressed the increase of intracellular calcium concentration ($[Ca^{2+}]_i$) caused by OGD/R in neurons.

CONCLUSIONS: These results demonstrate that BMSC-sEVs have significant neuroprotective effects against OGD/R-induced cell injury by suppressing oxidative stress and apoptosis, and Ca^{2+}/CaMK II signaling pathways may be involved in this process.

KEYWORDS: Oxygen-glucose deprivation and reperfusion; Cortical neurons; Oxidative stress; Small extracellular vesicles

World J Emerg Med 2021;12(1):61–67
DOI: 10.5847/wjem.j.1920-8642.2021.01.010

INTRODUCTION

Sudden cardiac arrest (CA) is critical for its high morbidity and mortality worldwide. Neurological injury after CA remains a major cause of poor prognosis among survivors.[1,2] Brain injury occurs not only during CA and resuscitation, but also after the reestablishment of brain reperfusion, namely ischemia/reperfusion (I/R) injury, which is a main target of neuroprotective treatments. Unfortunately, the treatment remains suboptimal. Cerebral I/R injury after the successful return of spontaneous circulation (ROSC) is a process driven by multiple mechanisms, including calcium overload, apoptosis, oxidative stress, and inflammation.[3] These mechanisms intersect with each other, discounting the effect of any single pharmacotherapy, even comprehensive interventions (like hypothermia).[4,5] Therefore, it is urgent to find a new, stable, and effective treatment.

© 2021 World Journal of Emergency Medicine

Multipotent mesenchymal stem cells (MSCs) play a role in neurovascular remodeling and neurological recovery following cerebral ischemia injury.[6,7] Rather than directly replacing parenchymal brain cells, the therapeutic mechanism of MSCs is suggested to produce extracellular vesicles (EVs) in a paracrine pattern. Small extracellular vesicles (sEVs), referring to 30–200 nm EVs, mainly including exosomes and microvesicles, are lipid bilayer-enclosed structures which contain a variety of cargos such as proteins, lipids, and DNA and RNA species, and participate in cell-to-cell signaling processes.[8] Previous studies have shown that sEVs from the bone marrow mesenchymal stem cells (BMSC-sEVs) play a protective role in myocardial and renal I/R injury.[9,10] However, how sEVs from MSCs protect the neuron cells in I/R is still not clear. In this study, we used oxygen-glucose deprivation and reperfusion (OGD/R) to establish a model of I/R in rat primary cortical neurons. Based on this model, we examined whether the mechanism through which BMSC-sEVs could rescue OGD/R-induced neuronal injury.

METHODS

Animals

Three-week-old male Sprague-Dawley (SD) rats weighing 50–60 g and fetal rats on embryonic days 17 and 18 (E17–18) were purchased from the Animal Experimental Center, Nanjing Medical University, China. All animal experiments were approved by the Institutional Animal Care and Use Committee (approval number: 1801008) of Nanjing Medical University, and carried out following the National Institutes of Health Guide for the Care and Use of Laboratory Animals.

Cell isolation and culture

BMSCs were harvested from the three-week-old SD rats. Briefly, the animals were given an intraperitoneal injection of chloral hydrate (300 mg/kg) for anesthesia before they were sacrificed. The marrow was flushed out after removing the epiphysis of femurs and tibias, followed by resuspension in low glucose Dulbecco's modified Eagle's medium (L-DMEM) (Gibco, USA). Twenty-four hours later, the medium was replaced to remove the non-adherent cells. Thereafter, the cells were harvested when they achieved 80%–90% confluence, followed by cell passage at a rate of 1:2. BMSCs from 3–4 passages were used for subsequent experiments.

Primary cortical neurons were cultured according to the previous description.[11] In brief, cerebral cortices were collected from the 17- to 18-day rat embryos. Dissected cortices were dissociated and suspended in the neurobasal medium containing 2 mmol glutamine and B27 (Invitrogen, USA), and then inoculated onto the plates coated with poly-L-lysine. All cells were cultured in an incubator with a humidified atmosphere of 5% CO_2 at 37 °C. The experiments were carried out at 8–9 days after the initial plating of cultures.

BMSC-sEVs purification and identification

BMSCs from the 3rd and the 4th passages at 70%–80% confluence were washed with phosphate-buffered saline (PBS) before incubation in L-DMEM containing 10% exosome-depleted fetal bovine serum (System Biosciences, USA). Forty-eight hours later, the medium was collected, while sEVs were isolated from the medium by multi-step centrifugation at 4 °C. In brief, the supernatants were filtered using a 0.22-μm filter, centrifuged for 30 minutes at 10,000*g* and ultra-centrifuged for 70 minutes at 110,000*g* (Beckman SW32 Ti) to pellet the sEVs. Finally, the sEVs were subjected to resuspension within 100 μL PBS and preserved under the temperature of –80 °C prior to utilization. The concentration of sEVs was determined through evaluating the contents of total protein by bicinchoninic acid (BCA) assay (Sigma-Aldrich, USA). The nanoparticle tracking analysis (NTA) (Malvern, UK) and the electron microscope were used to detect the BMSC-sEVs concentration, size distribution, and their specific markers CD9. Alix and heat shock protein 70 (HSP70) (Abcam, UK) were examined using the Western blot assay.

Internalization of BMSC-sEVs into cortical neurons

BMSC-sEVs were subjected to 5 minutes of PKH26 (Sigma-Aldrich, USA) labeling under the temperature of 37 °C in the dark in accordance with manufacturer protocols, and washed twice in PBS with centrifugation at 110,000*g* at 4 °C for 2 hours to remove unbound PKH26. Thereafter, the labeled sEVs (40 μg/mL) were added to the prepared cortical neurons for 24 hours. The nuclei were dyed using Hoechst33342 (Beyotime, China). The uptake of BMSC-sEVs by neurons was observed using a laser scanning confocal microscope (Olympus, Japan).

OGD/R

To achieve OGD, neurons were rinsed twice with PBS, cultured in glucose-free DMEM (Gibco, USA), and then put into an incubator containing 95% N_2 and 5% CO_2 at 37 °C for 2 hours. Then the cultures were incubated again in a normoxic incubator with normal culture medium for an additional 24 hours at 37 °C as reoxygenation (R).

Cells were divided into four groups, including the control group, OGD/R group, and OGD/R+sEVs groups (sEVs 20 μg/mL or 40 μg/mL). sEVs were added when initiating the reoxygenation process. Cells that were not exposed to OGD/R were defined as the control group.

Cell viability and lactate dehydrogenase (LDH) assays

After exposure to OGD/R, the cell viability was tested by cell counting kit-8 (CCK-8) (Beyotime, China), and the optical density was detected at the wavelength of 450 nm. The LDH cytotoxicity assay kit (Beyotime, China) was used to quantitatively evaluate neuron damage. Following OGD/R, the culture medium of cortical neurons was centrifuged to obtain the supernatants. The amount of LDH leakage was measured according to the manufacturer's instructions. The absorbance of the samples was measured spectrophotometrically at 490 nm. The results were expressed as the relative percentage of the control group.

Determination of mitochondrial membrane potential (MMP)

The tetrachloro-tetraethyl benzimidazol carbocyanine iodide fluorescent dye (JC-1) (Beyotime, China) was used to detect MMP. Briefly, cells were subjected to 20 minutes of JC-1 incubation in the dark at 37 °C. Meanwhile, the laser scanning confocal microscope was adopted to capture images. The ratio of JC-1 aggregates (red fluorescence) to monomers (green fluorescence) was calculated using ImageJ (NIH, USA). The loss of mitochondrial function was indicated by a decrease in the ratio of the red/green fluorescence intensity.[12]

Measurement of reactive oxygen species (ROS) generation, superoxide dismutase (SOD), and glutathione peroxidase (GPx)

Intracellular ROS was detected by an antioxidation-sensitive fluorescent probe 2',7'-dichlorodihydrofluorescein diacetate (DCFH-DA) (Beyotime, China). The neurons were washed and then incubated with 10 μmol DCFH-DA at 37 °C for 20 minutes with gentle shaking. The fluorescence intensity was quantified using a fluorospectrophotometer at an excitation wavelength of 485 nm and an emission wavelength of 525 nm. After exposure to OGD/R, the neurons were harvested, sonicated, and centrifuged to collect the supernatants. The levels of SOD and GPx were determined with the respective assay kits (Beyotime, China) according to manufacturers' instructions.

Measurement of intracellular calcium concentration ($[Ca^{2+}]_i$)

Neurons were washed by PBS and incubated with the complete medium containing 5 μmol Fluo-4 acetoxymethyl (AM) (KeyGen Biotech, China) for 30 minutes in the dark at 37 °C. Subsequently, the cells were washed with PBS and incubated at 37 °C for another 10 minutes prior to measurement. Finally, the fluorescence was analyzed by flow cytometry (BD Biosciences, USA) at an excitation wavelength of 488 nm and an emission wavelength of 530 nm, and the relative mean fluorescence intensity of Fluo-4 was used to indicate the $[Ca^{2+}]_i$.

Terminal deoxynucleotidyl transferase (TdT)-mediated dUTP nick end labeling (TUNEL) staining

After treatment, neurons were stained with TUNEL dye (Roche, USA) according to the manufacturer's recommendations. Then, 4',6-diamidino-2-phenylindole (DAPI) (Beyotime, China) was used as the nuclear counterstain. Fluorescence images were acquired with the laser scanning confocal microscope (Olympus, Japan), and TUNEL-positive nuclei of five non-overlapping fields per coverslip were counted. The apoptotic index was expressed as the percentage of the ratio of TUNEL-positive nucleus count to the total nucleus number determined by DAPI counterstaining.

Western blot analysis

Equal amounts of protein were loaded onto 12% sodium dodecyl sulfate-polyacrylamide gels and transferred onto the polyvinylidene fluoride (PVDF) membranes (Millipore Corporation, USA). Afterwards, the membranes were blocked and followed by incubation with primary antibodies at 4 °C overnight. The primary antibodies used were anti-cleaved caspase-3 antibody (1:1,000; Cell Signaling Technology, USA), anti-B-cell lymphoma 2 (Bcl-2) (Abcam, UK), anti-Bcl-2-associated X (Bax) (Cell Signaling Technology, USA), anti-glyceraldehyde-3-phosphate dehydrogenase (GAPDH) (Cell Signaling Technology, USA), anti-calcium/calmodulin-dependent kinase II (CaMK II) (Cell Signaling Technology, USA), and anti-phosphorylated CaMK II (p-CaMK II) (Abcam, UK). Then, the membranes were further incubated with the appropriate horseradish peroxidase-conjugated secondary antibodies at room temperature for 2 hours, and the resultant protein bands were visualized by enhanced chemiluminescence (Beyotime, China).

Statistical analysis

Data were expressed as the mean±standard deviation (SD) for all parameters. Differences between the two

groups were analyzed by Student's *t*-test. Multiple comparisons were performed with one-way analysis of variance (ANOVA) followed by the Tukey post-hoc test. All calculations were performed using GraphPad Prism software version 6.0 (GraphPad, CA, USA). The *P*-value <0.05 was considered statistically significant.

RESULTS

Identification of BMSCs and BMSC-sEVs

The BMSCs appeared as fibroblast-like and spindle-shaped swirling adherent cells under the phase-contrast microscope (Figure 1A). For assessing their differentiation, the cells were induced by the specific medium. BMSCs successfully differentiated into osteoblasts and adipocytes at three to four weeks after induction by osteogenic medium and adipogenic medium, respectively (Figure 1B). The results of transmission electron microscopy showed that the isolated sEVs displayed a bilayer membrane (Figure 1C). The NTA showed that the diameters of the particles were within the range of 50–150 nm, averaging 104 nm (Figure 1D). Furthermore, three specific surface markers (Alix, Hsp70, and CD9) were detected in BMSC-sEVs (Figure 1E). The PKH26 (red)-labeled sEVs swarmed into the neurons to the perinuclear cytoplasm within 24 hours (Figure 1F).

BMSC-sEVs protected primary cortical neurons against OGD/R-induced injury

The OGD/R exposure significantly decreased the cell viability and increased the LDH leakage, which was strikingly attenuated by BMSC-sEVs, suggesting that BMSC-sEVs can dependently attenuate OGD/R-induced cell injury in primary cortical neurons (Figures 2A, B).

BMSC-sEVs alleviated OGD/R-induced oxidative stress in primary cortical neurons

The OGD/R exposure dramatically reduced the red/green fluorescence intensity of JC-1, suggesting a significant decrease of MMP, but this decrease was inhibited after the treatment of BMSC-sEVs (Figure 2C). Additionally, OGD/R exposure resulted in a 4-fold increase in cellular ROS level. Compared to the control group, the levels of SOD and GPx decreased in OGD/R group, and as speculated, BMSC-sEV treatment obviously attenuated OGD/R-induced ROS generation, and enhanced SOD and GPx activities in rat primary cortical neurons. Taken together, BMSC-sEV treatment can suppress OGD/R-induced oxidative stress *in vitro* (Figures 2D, E, and F).

BMSC-sEVs reduced OGD/R-induced apoptosis in primary cortical neurons

The TUNEL staining assay was performed to assess the

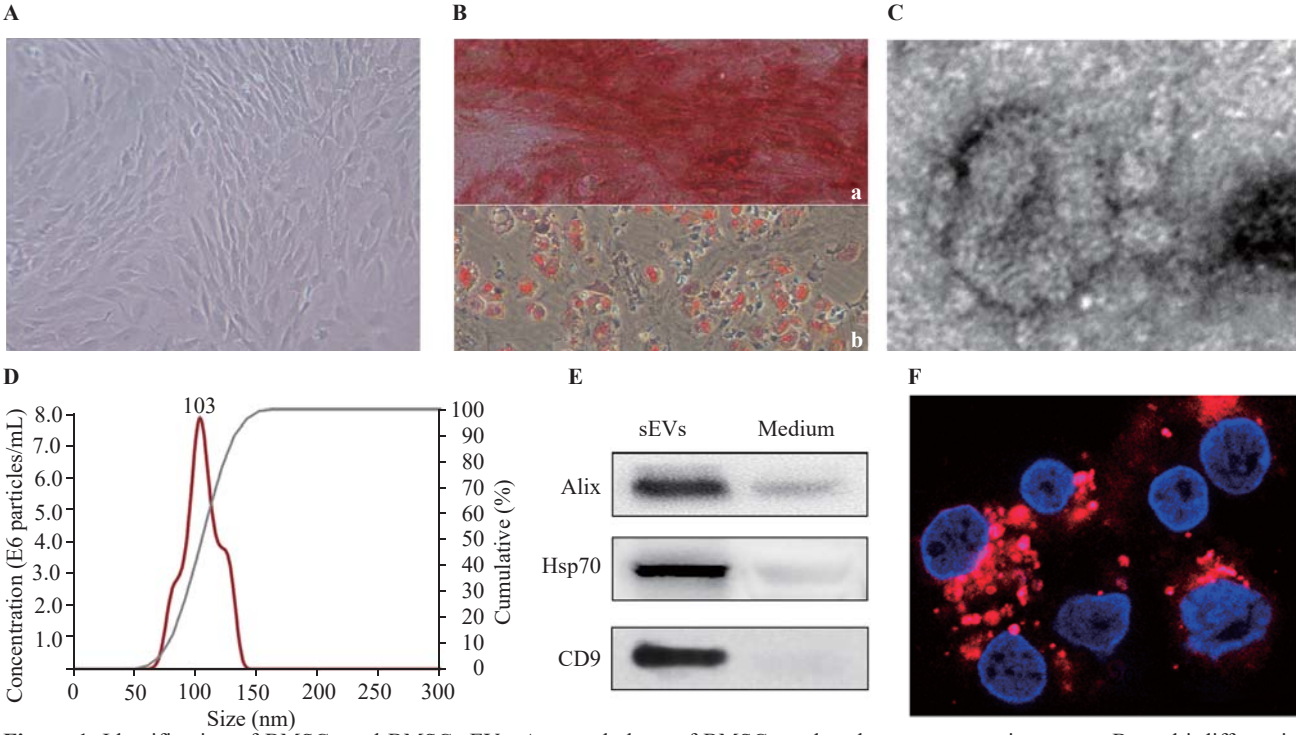

Figure 1. Identification of BMSCs and BMSC-sEVs. A: morphology of BMSCs under phase-contrast microscope; B: multi-differentiation potential of BMSCs; a: Alizarin Red staining of osteogenic mineralization; b: Oil Red O staining of small lipid droplets (bar=100 μm); C: transmission electron micrograph of BMSC-sEVs (bar=50 nm); D: nanoparticle tracking analysis of sEVs; E: the expression of Alix, Hsp70, CD9 in conditioned medium and sEVs by Western blot assay; F: the uptake of PKH26-labeled sEVs (red) by neurons (4',6-diamidino-2-phenylindole [DAPI] blue) at 24 hours (bar=20 μm); BMSCs: bone marrow mesenchymal stem cells; sEVs: small extracellular vesicles.

percentage of apoptotic cells. After OGD/R exposure, the TUNEL-positive cells in OGD/R group were significantly increased, while BMSC-sEVs substantially attenuated OGD/R-induced apoptosis, as evidenced by the diminishing TUNEL-positive cells (Figures 3A, B). The protein levels of the apoptosis-associated cleaved caspase-3, Bcl-2, and Bax were measured by Western blot assay. OGD/R increased the cleaved caspase-3 level and decreased the Bcl-2/Bax ratio. These changes were remarkably reversed by BMSC-sEVs, manifested as rising Bcl-2/Bax ratio and falling cleaved caspase-3/GAPDH ratio (Figure 3C).

BMSC-sEV treatment suppressed OGD/R-induced Ca^{2+}/CaMK II signaling in primary cortical neurons

We explored whether Ca^{2+}/CaMK II signaling pathway was involved in the neuroprotective effects of BMSC-sEVs. Western blot analysis showed that the level of p-CaMK II protein was up-regulated by OGD/R exposure, but was dose-dependently down-regulated by BMSC-sEV treatment at concentrations of 20 and 40 μg/mL (Figure 3D). At the same time, BMSC-sEVs suppressed OGD/R-induced elevation of $[Ca^{2+}]_i$ (Figure 3E), implying that sEVs may reduce OGD/R-induced Ca^{2+}/CaMK II activation in cortical neurons.

DISCUSSION

A previous study[13] has confirmed that instead of directly reaching the locus of brain injury, MSCs mainly play their therapeutic role relying on their paracrine properties. SEVs have been recognized as important messengers in intercellular communication that act on target cells via transporting bioactive lipids, proteins, and RNAs.[8,14] BMSC-sEVs have been identified as neuroprotective candidates in hypoxia-ischemia brain disease by several studies,[15,16] but no mechanisms have been clarified to explain the protective effects of BMSC-sEVs on I/R-induced neuronal injury.

Brain damages, caused by CA and ROSC, including

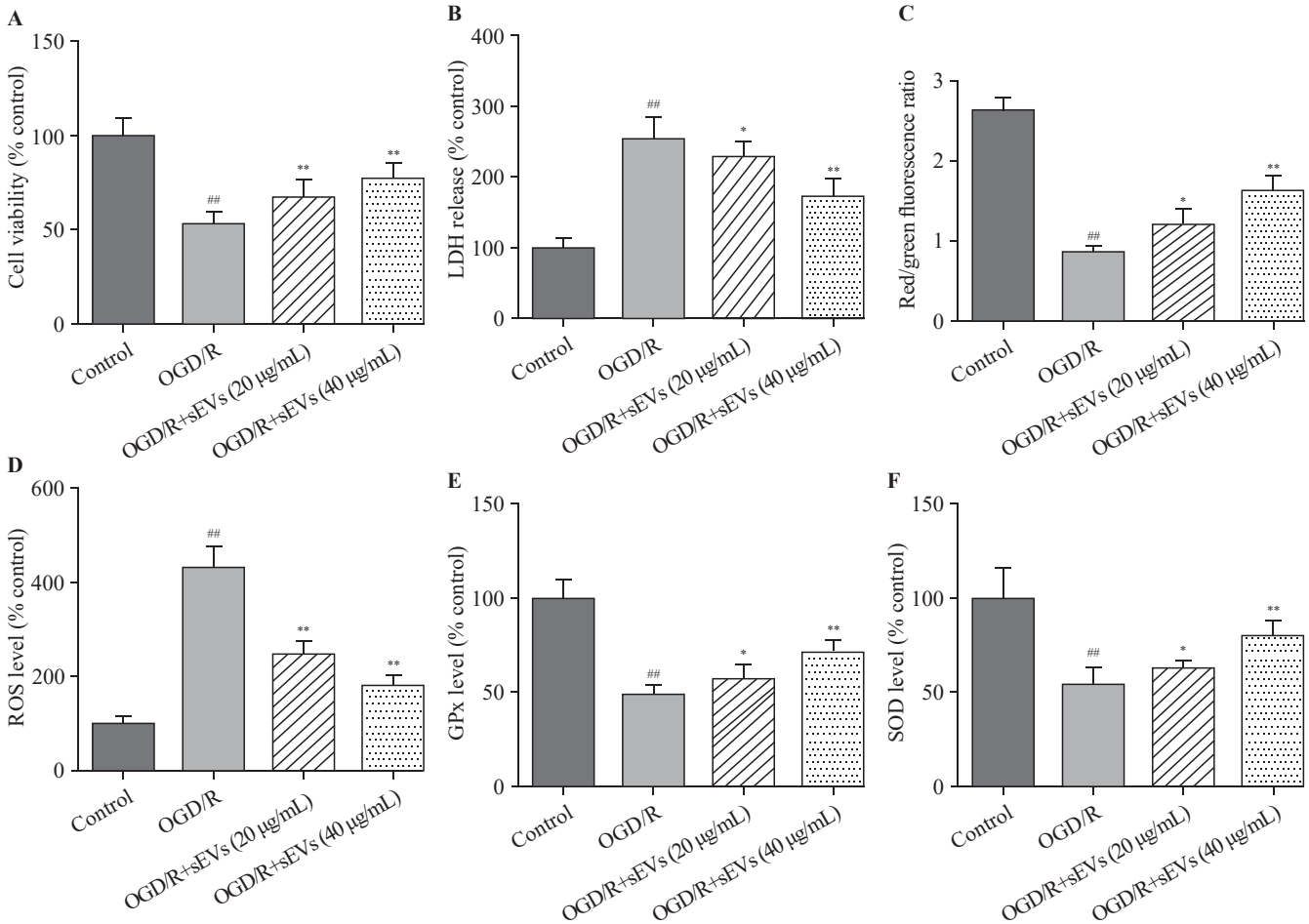

Figure 2. Effects of BMSC-sEVs on OGD/R-induced neuronal injury and oxidative stress. A: cell viability measured by cell counting kit-8 assay; B: cytotoxicity assessed by lactate dehydrogenase (LDH) assay; C, D, E, and F: levels of oxidative status markers including mitochondrial membrane potential (MMP), reactive oxygen species (ROS) generation, glutathione peroxidase (GPx), and superoxide dismutase (SOD) determined using respective assay kits; BMSCs: bone marrow mesenchymal stem cells; sEVs: small extracellular vesicles; OGD/R: oxygen-glucose deprivation and reperfusion; compared with the control group, $^{\#\#}P<0.01$; compared with the OGD/R group, $^{*}P<0.05$, $^{**}P<0.01$.

complete temporary global cerebral ischemia and secondary I/R injury, are complex processes associated with oxidative stress, intracellular Ca^{2+} overload, inflammation, and apoptosis, all leading to cell death. In our study, BMSC-sEVs attenuated OGD/R-induced neuronal viability and inhibited LDH release, indicating that BMSC-sEVs have a protective effect on OGD/R-induced neuronal damage. Our data also showed that BMSC-sEV treatment significantly antagonized cell injury under OGD/R by inhibiting cell apoptosis. Mitochondria are the main organella initiating oxidative stress. Mitochondrial dysfunction is manifested as the decrease in MMP and the overproduction of ROS.[17] Our data demonstrated that the treatment with BMSC-sEVs suppressed oxidative stress by decreasing ROS production, increasing SOD activity, and strengthening GPx activity in primary rat cortical neurons after OGD/R. These findings are similar to a previous study in that BMSC-sEVs can protect H9C2 cardiomyocytes against H_2O_2-induced I/R injury by attenuating ROS production and apoptosis.[9] Furthermore, mitochondrial depolarization was observed in neurons after OGD/R, and BMSC-sEVs prevented OGD/R-induced MMP dissipation. Thus, we may conclude that the protective effects of BMSC-sEVs against OGD/R-induced neuron injury are dependent on enhanced mitochondrial function, anti-oxidative stress, and anti-apoptosis.

To further explore the signaling pathways in the neuroprotective effects of BMSC-sEVs, we examined the level of $[Ca^{2+}]_i$ and activation of CaMK II protein. CaMK II, a major highly expressed multifunctional Ser/Thr kinase in neuronal tissues, plays a crucial role in a variety of processes, including oxidative stress,[18] apoptosis,[19] axonal and dendritic arborization as well as synaptogenesis.[20] As a second messenger, Ca^{2+} is involved in numerous cellular processes; therefore, Ca^{2+} signaling disturbance may evoke neuronal damage.[21] When the $[Ca^{2+}]_i$ increases, Ca^{2+} binds to calmodulin (CaM), and then Ca^{2+}/CaM complex interacts with target proteins to initiate various processes, like the activation of CaMK II.[22] As shown in our study, OGD/R exposure significantly increased the levels of p-CaMK II/CaMK II, but the administration of BMSC-sEVs suppressed the levels of p-CaMK II/CaMK II. This finding was consistent with that of a previous study, which showed that decreasing the expression of p-CaMK II could counter neuronal injury induced by I/R *in vivo*.[23] Considering the association between CaMK II and $[Ca^{2+}]_i$, we used the Fluo-4 AM probe to detect Ca^{2+} fluorescence intensity in neurons, and found that Ca^{2+} fluorescence intensity increased in response to oxidative stress under OGD/R, and decreased after BMSC-sEV treatment. This finding supported the anti-apoptotic effects of BMSC-

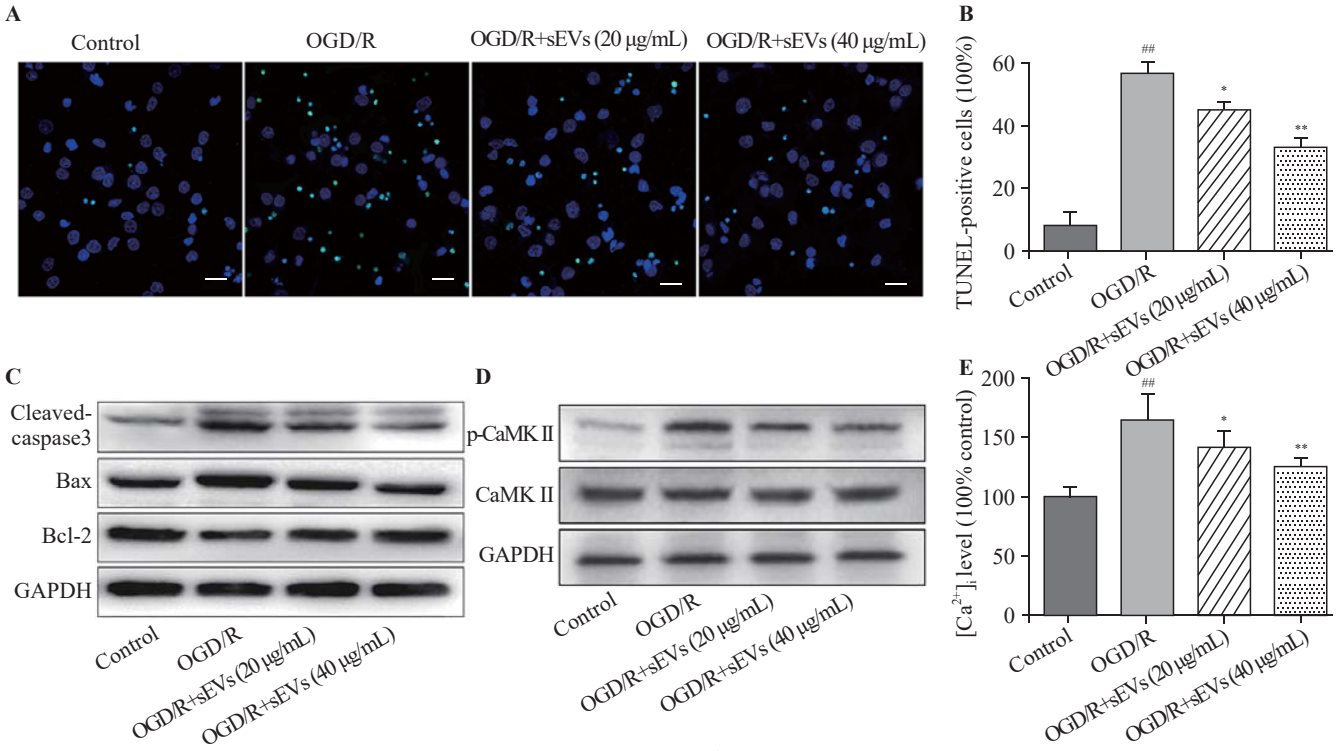

Figure 3. Effects of BMSC-sEVs on OGD/R-induced neuronal apoptosis and Ca^{2+}/CaMK II signaling pathway. Representative TUNEL images (A) and quantification of TUNEL-positive cells (B) (bar=20 μm); C: the protein levels of cleaved caspase-3, Bax and Bcl-2 determined by Western blot assay; D: the protein levels of CaMK II and p-CaMK II were determined by Western blot assay; E: the relative fluorescent intensity of Fluo-4 used to indicate the $[Ca^{2+}]_i$ quantity; BMSCs: bone marrow mesenchymal stem cells; sEVs: small extracellular vesicles; OGD/R: oxygen-glucose deprivation and reperfusion; compared with control group, $^{\#\#}P<0.01$; compared with OGD/R group, $^{*}P<0.05$, $^{**}P<0.01$.

sEVs on cardiac stem cells in that BMSC-sEVs could restrain oxidative damage and apoptosis by targeting Ca^{2+}/CaMK II.[24] Our data revealed that BMSC-sEV treatment suppressed OGD/R-induced oxidative stress and apoptosis via Ca^{2+}/CaMK II pathway in primary rat cortical neurons.

CONCLUSIONS

The study reveals that BMSC-sEVs protect rat cortical neurons from I/R injury which may be attributed to its anti-oxidant and anti-apoptosis activities via Ca^{2+}/CaMK II pathway. Thus, BMSC-sEVs might be a therapeutic target for cerebral I/R injury after successful ROSC.

Funding: This work was supported by the Natural Science Foundation of China (81701872) and Medical Innovation Teams of Jiangsu Province (CXTDA2017007).

Ethical approval: All animal experiments were approved by the Institutional Animal Care and Use Committee (IACUC, Approval number: 1801008) of Nanjing Medical University.

Conflicts of interest: The authors indicated no potential conflicts of interest.

Contributors: SSG and XWK contributed equally to this study. All authors reviewed and approved the final version of manuscript for publication.

REFERENCES

1 Matthews EA, Magid-Bernstein J, Presciutti A, Rodriguez A, Roh D, Park S, et al. Categorization of survival and death after cardiac arrest. Resuscitation. 2017;114:79-82.
2 Rossetti AO, Rabinstein AA, Oddo M. Neurological prognostication of outcome in patients in coma after cardiac arrest. Lancet Neurol. 2016;15(6):597-609.
3 Halhalli HC, Özbek AE, Çelİk E, Yİğİt Y, Yilmaz S, Çardak M. Benefits of using an endotracheal tube introducer as an adjunct to a Macintosh laryngoscope for endotracheal intubation performed by inexperienced doctors during mechanical CPR: A randomized prospective crossover study. World J Emerg Med. 2019;10(3):182-6.
4 Chan PS, Berg RA, Tang Y, Curtis LH, Spertus JA. Association between therapeutic hypothermia and survival after in-hospital cardiac arrest. JAMA. 2016;316(13):1375-82.
5 Geocadin R, Tahsili-Fahadan P, Farrokh S. Hypothermia and brain inflammation after cardiac arrest. Brain Circ. 2018;4(1):1-13.
6 Steinberg GK, Kondziolka D, Wechsler LR, Lunsford LD, Coburn ML, Billigen JB, et al. Clinical outcomes of transplanted modified bone marrow-derived mesenchymal stem cells in stroke: a phase 1/2a study. Stroke. 2016;47(7):1817-24.
7 Chung TN, Kim JH, Choi BY, Jeong JY, Chung SP, Kwon SW, et al. Effect of adipose-derived mesenchymal stem cell administration and mild hypothermia induction on delayed neuronal death after transient global cerebral ischemia. Crit Care Med. 2017;45(5):e508-15.
8 Mathieu M, Martin-Jaular L, Lavieu G, Thery C. Specificities of secretion and uptake of exosomes and other extracellular vesicles for cell-to-cell communication. Nat Cell Biol. 2019;21(1):9-17.
9 Liu L, Jin X, Hu CF, Li R, Zhou Z, Shen CX. Exosomes derived from mesenchymal stem cells rescue myocardial ischaemia/reperfusion injury by inducing cardiomyocyte autophagy via AMPK and Akt pathways. Cell Physiol Biochem. 2017;43(1):52-68.
10 Li L, Wang R, Jia Y, Rong R, Xu M, Zhu T. Exosomes derived from mesenchymal stem cells ameliorate renal ischemic-reperfusion injury through inhibiting inflammation and cell apoptosis. Front Med (Lausanne). 2019;6:269.
11 Xu L, Cao H, Xie Y, Zhang Y, Du M, Xu X, et al. Exosome-shuttled miR-92b-3p from ischemic preconditioned astrocytes protects neurons against oxygen and glucose deprivation. Brain Res. 2019;1717:66-73.
12 Xia R, Ji C, Zhang L. Neuroprotective effects of pycnogenol against oxygen-glucose deprivation/reoxygenation-induced injury in primary rat astrocytes via NF-kappa B and ERK1/2 MAPK pathways. Cell Physiol Biochem. 2017;42(3):987-98.
13 Teixeira FG, Carvalho MM, Sousa N, Salgado AJ. Mesenchymal stem cells secretome: a new paradigm for central nervous system regeneration? Cell Mol Life Sci. 2013;70(20):3871-82.
14 Keshtkar S, Azarpira N, Ghahremani MH. Mesenchymal stem cell-derived extracellular vesicles: novel frontiers in regenerative medicine. Stem Cell Res Ther. 2018;9(1):63.
15 Deng M, Xiao H, Zhang H, Peng H, Yuan H, Xu Y, et al. Mesenchymal stem cell-derived extracellular vesicles ameliorate hippocampal synaptic impairment after transient global ischemia. Front Cell Neurosci. 2017;11:205.
16 Xin H, Katakowski M, Wang F, Qian JY, Liu XS, Ali MM, et al. MicroRNA cluster miR-17-92 cluster in exosomes enhance neuroplasticity and functional recovery after stroke in rats. Stroke. 2017;48(3):747-53.
17 Gong Z, Pan J, Shen Q, Li M, Peng Y. Mitochondrial dysfunction induces NLRP3 inflammasome activation during cerebral ischemia/reperfusion injury. J Neuroinflammation. 2018;15(1):242.
18 Bracken C, Beauverger P, Duclos O, Russo RJ, Rogers KA, Husson H, et al. CaMK II as a pathological mediator of ER stress, oxidative stress, and mitochondrial dysfunction in a murine model of nephronophthisis. Am J Physiol Renal Physiol. 2016;310(11):F1414-22.
19 Li C, Li L, Lin B, Fang Y, Yang H, Liu H, et al. Tris (1,3-dichloro-2-propyl) phosphate induces toxicity by stimulating CaMK 2 in PC12 cells. Environ Toxicol. 2017;32(6):1784-91.
20 Mockett BG, Guevremont D, Wutte M, Hulme SR, Williams JM, Abraham WC. Calcium/calmodulin-dependent protein kinase II mediates group I metabotropic glutamate receptor-dependent protein synthesis and long-term depression in rat hippocampus. J Neurosci. 2011;31(20):7380-91.
21 Neher E, Sakaba T. Multiple roles of calcium ions in the regulation of neurotransmitter release. Neuron. 2008;59(6):861-72.
22 Wayman GA, Lee YS, Tokumitsu H, Silva AJ, Soderling TR. Calmodulin-kinases: modulators of neuronal development and plasticity. Neuron. 2008;59(6):914-31.
23 Zhu MX, Lu C, Xia CM, Qiao ZW, Zhu DN. Simvastatin pretreatment protects cerebrum from neuronal injury by decreasing the expressions of phosphor-CaMK II and AQP4 in ischemic stroke rats. J Mol Neurosci. 2014;54(4):591-601.
24 Wang Y, Zhao R, Liu D, Deng W, Xu G, Liu W, et al. Exosomes derived from miR-214-enriched bone marrow-derived mesenchymal stem cells regulate oxidative damage in cardiac stem cells by targeting CaMK II. Oxid Med Cell Longev. 2018;2018:4971261.

Received March 29, 2020
Accepted after revision September 20, 2020